# Expression, purification, crystallization and preliminary X-ray diffraction studies of phosphoglycerate mutase from *Staphylococcus aureus* NCTC8325

Amlan Roychowdhury, Anirban Kundu, Akanksha Gujar, Madhuparna Bose and Amit Kumar Das*

Department of Biotechnology, Indian Institute of Technology Kharagpur, Kharagpur 721 302, India

Correspondence e-mail: amitk@hijli.iitkgp.ernet.in

Phosphoglycerate mutase (PGM) is a key enzyme in carbohydrate metabolism. It takes part in both glycolysis and gluconeogenesis. PGM from pathogenic *Staphylococcus aureus* (NCTC8325) was cloned in pQE30 expression vector overexpressed in *Escherichia coli* M15 (pREP4) cells and purified to homogeneity. The protein was crystallized from two different conditions, (i) 0.1 *M* HEPES pH 7.5, 20%(*w/v*) polyethylene glycol 10 000 and (ii) 0.2 *M* NaCl, 0.1 *M* bis-tris pH 6.5, 25%(*w/v*) polyethylene glycol 3350, at 25°C by the sitting-drop vapour-diffusion method. Crystals grown at pH 7.5 diffracted to 2.5 Å resolution and belonged to the orthorhombic space group $P2_12_12$, with unit-cell parameters $a = 77.0$, $b = 86.11$, $c = 94.07$ Å. Crystals from the second condition at pH 6.5 diffracted to 2.00 Å resolution. These crystals belonged to the orthorhombic space group $P2_12_12_1$, with unit-cell parameters $a = 73.21$, $b = 81.75$, $c = 89.18$ Å. X-ray diffraction data have been collected and processed to the maximum resolution to determine the structure of PGM. The structure has been solved by molecular replacement and structure refinement is now in progress.

1. Introduction

Drug-resistant *Staphylococcus aureus* has become a potent threat to modern medical practice. Its ability to form biofilms has increased its menace (Götz, 2002). As an opportunistic pathogen, it may cause conditions ranging from minor skin infections to life-threatening diseases such as endocarditis and osteomyelitis (Archer, 1998). Recent studies have shown that a handful of enzymes which participate in glycolysis are also involved in pathogenesis (Purves *et al.*, 2010) and in the formation of biofilms resulting in reduced anti-microbial susceptibility (Becker *et al.*, 2001).

Amongst many other glycolytic enzymes, the ubiquitous enzyme phosphoglycerate mutase (PGM) catalyzes the reversible conversion of 3-phosphoglycerate (3PGA) to 2-phosphoglycerate (2PGA). There are two subgroups of PGMs: the cofactor-dependent PGMs (dPGMs), which require 2,3-diphosphoglyceric acid (DPG) as a phosphate-group donor, and the cofactor-independent PGMs (iPGMs). dPGMs (EC 5.4.2.11) are ubiquitous among vertebrates (including humans), certain invertebrates, fungi and some bacteria, primarily Gram-negative bacteria. iPGMs (EC 5.4.2.12) are predominant in higher plants, some invertebrates, fungi, algae and Gram-positive bacteria such as *Bacillus*, *Clostridium*, *Staphylococcus* and *Streptococcus* species. However, *Staphylococcus* species also contain two isoforms of dPGM. Unlike dPGMs, iPGMs function as monomers of ∼60 kDa and exhibit no significant sequence homology to dPGMs. iPGMs share a distant relation to alkaline phosphatases in the region of the metal-binding site. Another unique feature of iPGMs is the absolute and specific requirement for Mn^{2+} ions for the formation of the phospho-enzyme reaction intermediate on a serine residue in the active site of iPGM. The Mn^{2+}-dependent activity of iPGMs differs from the activity of other Mn^{2+}-dependent enzymes in that iPGMs utilize the ions in an extremely pH-sensitive manner in the pH range 6.0–8.0 (Kuhn *et al.*, 1995). This pH dependence is extremely important for the regulation of iPGM activity in the sporulation process of Gram-positive bacteria (Magill *et al.*, 1994, 1996). Structural analysis of iPGMs revealed that the bi-domain enzyme iPGM requires precise orientation of the substrate in the active site and the formation of coordination bonds to Mn^{2+} ions (Nukui *et al.*, 2007;
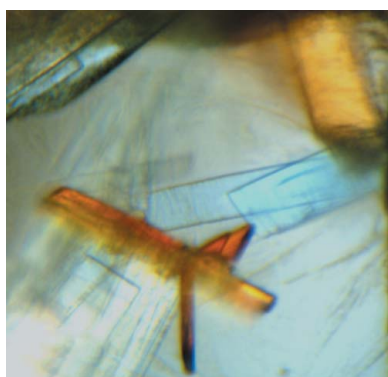
Jedrzejas *et al.*, 2000) by three histidines. Thus, pH-dependent change in the coordination geometry of Mn^{2+} ions results in inhibition of the enzyme. The apparent absence of iPGM in vertebrates, including humans, and its importance in some Gram-positive bacteria have made this class of enzyme an excellent target for antibacterial drugs.

S. aureus NCTC8325 contains a single iPGM (Sa-iPGM) of 505 amino acids and little is known about its role in the pathogenesis of this Gram-positive coccus. It is also evident that glycolytic enzymes interact with each other in eukaryotic cells. The interactions between different glycolytic enzymes have been strongly established by both biophysical and kinetic experiments (MacGregor *et al.*, 1980; Weber & Bernhard, 1982; Ovádi & Keleti, 1978). In prokaryotes, such intermolecular interactions between glycolytic enzymes have not yet been reported. However, in *Thermotoga maritima* the two glycolytic enzymes phosphoglycerate kinase (PGK) and triosephosphate isomerase (TIM) are expressed as a tetrameric fusion protein (Schurig *et al.*, 1995). The existence of such a bifunctional enzyme may reinforce the concept that in prokaryotes the glycolytic enzymes interact and form supramolecular complexes. Structures of PGK (PDB entry 4dg5; Roychowdhury *et al.*, 2011), GAPDH (Mukherjee *et al.*, 2010) and TIM (Mukherjee *et al.*, 2012) from *S. aureus* have already been solved. These are the essential prerequisites for study of structure-based interaction. Therefore, structural analysis of staphylococcal iPGM and its complexes with other enzymes will certainly aid in elucidating its mode of interaction and the detailed mechanism of its catalysis. Hence, we have focused our attention on structural and mechanistic studies of this important enzyme, and the present work reports the cloning, overexpression, purification, crystallization and preliminary X-ray diffraction analysis of Sa-iPGM.

2. Materials and methods

2.1. Cloning

The sequences corresponding to the open reading frame of Sa-iPGM (UniProt ID Q2G029) were amplified by polymerase chain reaction from the NCTC8325 genomic DNA as the template, using the sequence-specific primer pair 5′-CG**GGATCC**ATGGCTAAGA-AACCAACTGCG-3′ (forward primer with a *Bam*HI recognition site) and 5′-GG**GGTACC**TTAGTGTTTAATTAAAGATTCACC-3′ (reverse primer with a *Kpn*I recognition site). The purified and restriction-digested PCR product was subsequently cloned into the *Bam*HI- and *Kpn*I-digested pQE30 expression vector (Qiagen, USA). The recombinant DNA was then transformed into chemically competent *Escherichia coli* M15 (pREP4) cells for IPTG-induced overexpression and subsequently selected on ampicillin/kanamycin plates. The positive clones were verified by DNA sequencing.

2.2. Overexpression and purification

The recombinant expression of Sa-iPGM was performed by growing transformed cells in Luria–Bertani broth at 37°C containing ampicillin (100 μg ml^{-1}) and kanamycin (25 μg ml^{-1}). Recombinant cell mass was induced with 100 μ*M* IPTG when the OD_{600} reached 0.6 and was grown for 4 h at the same temperature. Harvested cells from 2 l culture were resuspended and lysed by ultrasonication in buffer *A* (10 m*M* Tris–HCl pH 8.0, 10 m*M* imidazole, 300 m*M* NaCl) containing leupeptin, pepstatin, aprotinin (0.1 μ*M* each) and 0.2 μ*M* phenylmethylsulfonyl chloride (PMSF) as protease inhibitors. The lysate was centrifuged at 22 000*g* at 4°C for 40 min. The supernatant was loaded onto Ni–NTA Sepharose High Performance affinity matrix (GE Healthcare Biosciences) pre-equilibrated with buffer *A*. The column was then washed extensively with buffer *A* to remove

bound contaminants. Recombinant His$_6$-tagged Sa-iPGM was finally eluted with buffer *B* (10 m*M* Tris–HCl pH 8.0, 300 m*M* NaCl, 50 m*M* imidazole). The eluted protein was subjected to size-exclusion chromatography using Superdex 200 prep-grade matrix in a C 16/70 column (GE Healthcare Biosciences) equilibrated with buffer *C* (10 m*M* Tris–HCl pH 8.0, 50 m*M* NaCl, 5 μ*M* MnCl$_2$, 1 m*M* DTT) on an ÄKTAprime plus system (GE Healthcare Biosciences). 2 ml fractions were collected at a flow rate of 1 ml min^{-1}. The protein was only obtained in monomeric form and the fractions containing the desired protein were pooled together. The protein concentration was estimated by the method of Bradford (1976) and the purity was verified by 12% SDS–PAGE.

2.3. Crystallization

The protein was purified and concentrated to 36.0 mg ml^{-1} using an Amicon Ultra concentrator (10 kDa molecular-weight cutoff, Millipore). Droplets of 1.5 μl concentrated protein solution in buffer *C* were mixed with an equal volume of reservoir solution and equilibrated against 100 μl reservoir solution in a 96-well CrystalEX
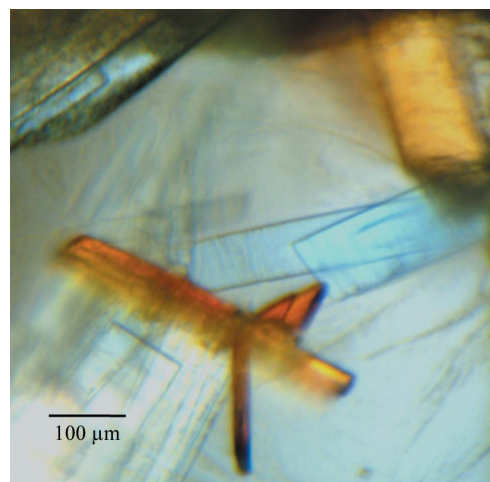
(*a*)
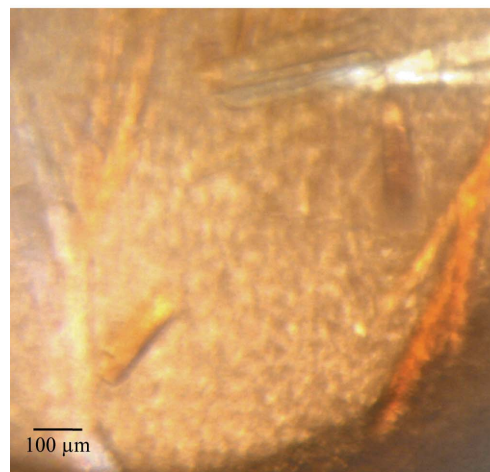
(*b*)

Figure 1
Crystals of Sa-iPGM. (*a*) The crystals obtained from 0.1 *M* HEPES pH 7.5, 20%(*w/v*) polyethylene glycol 10 000 (condition No. 38 from Crystal Screen 2, Hampton Research) using the sitting-drop vapour-diffusion method at 25°C measured 0.3 × 0.1 × 0.015 mm. (*b*) The crystals of Sa-iPGM grown from 0.2 *M* NaCl, 0.1 *M* bis-tris pH 6.5, 25%(*w/v*) polyethylene glycol 3350 (condition No. 71 from Index) by the sitting-drop vapour-diffusion method at 25°C measured 0.2 × 0.06 × 0.045 mm.

sitting-drop plate (Corning) using sparse-matrix screens from Hampton Research (Crystal Screen, Crystal Screen 2 and Index) at 25°C. Rectangular plate-shaped crystals arranged in a bunch were found in two different conditions. Sa-iPGM crystals were grown in the presence of (i) 0.1 M HEPES pH 7.5, 20%(w/v) polyethylene glycol 10 000 (condition No. 38 from Crystal Screen 2) and (ii) 0.2 M NaCl, 0.1 M bis-tris pH 6.5, 25%(w/v) polyethylene glycol 3350 (condition No. 71 from Index).
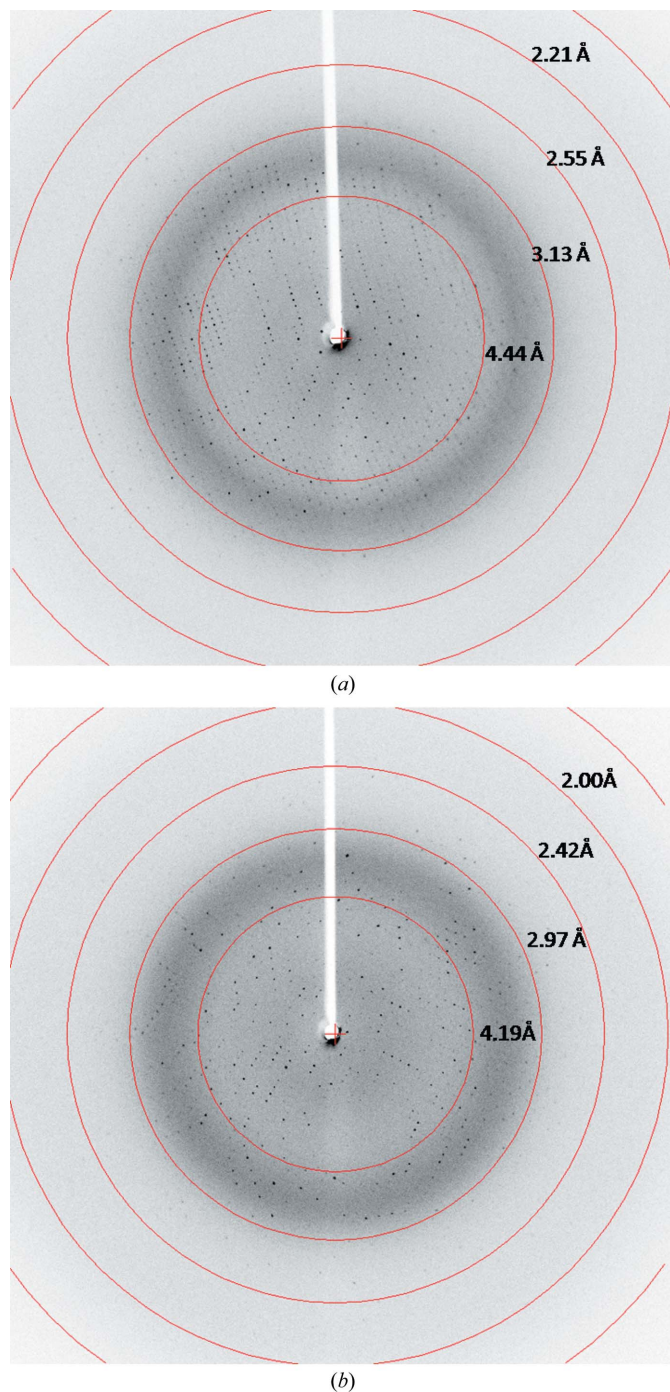

(a)

(b)

Figure 2
Diffraction patterns of Sa-iPGM. (a) Diffraction image collected from the crystal grown in condition (i); the oscillation width and the exposure time for each frame were 1° and 3 min, respectively. (b) Diffraction image collected from the crystal grown in condition (ii); the oscillation width and the exposure time for each frame were 0.5° and 2 min, respectively.

Table 1
Data-collection and processing statistics.

Values in parentheses are for the outermost resolution shell.

	Crystal (i)	Crystal (ii)
Wavelength (Å)	1.5418	1.5418
Exposure time (min)	3	2
Space group	$P2_12_12$	$P2_12_12_1$
Unit-cell parameters (Å)	$a = 77.00, b = 86.11, c = 94.07$	$a = 73.21, b = 81.75, c = 89.18$
Mosaicity (°)	0.289	0.196
Matthews coefficient (V_M) (Å^3 Da^{-1})	2.76	2.36
Solvent content (%)	55.5	48.0
Monomers per asymmetric unit (Z)	1	1
Resolution range (Å)	19.57–2.5 (2.64–2.50)	19.68–2.0 (2.11–2.00)
Total No. of observations	318788 (45289)	255212 (29553)
No. of unique reflections	22052 (3145)	36463 (5068)
Multiplicity	14.5 (14.4)	7.0 (5.8)
Completeness (%)	99.4 (98.8)	99.3 (95.7)
Average $I/\sigma(I)$	22.5 (4.4)	21.7 (3.8)
$R_{r.i.m.}$† (%)	14.8 (84.9)	9.0 (51.1)
R_{merge}‡ (%)	14.4 (82.1)	8.3 (46.5)
$CC_{1/2}$	99.9 (96.2)	99.9 (87.8)

† $R_{r.i.m.} = \sum_{hkl}\{N(hkl)/[N(hkl)-1]\}^{1/2}\sum_i|I_i(hkl)-\langle I(hkl)\rangle|/\sum_{hkl}\sum_i I_i(hkl)$.
‡ $R_{merge} = \sum_{hkl}\sum_i|I_i(hkl)-\langle I(hkl)\rangle|/\sum_{hkl}\sum_i I_i(hkl)$, where $I_i(hkl)$ is the intensity of the ith observation of reflection hkl.

2.4. Data collection

The diffraction data were collected at our home source: a Rigaku MicroMax-007 HF microfocus rotating-anode X-ray generator (Cu $K\alpha$, λ = 1.5418 Å) equipped with a Rigaku R-AXIS IV^{++} detector (Rigaku Americas Corporation). Single crystals were cryoprotected using 5%(v/v) glycerol in reservoir solution and were flash-cooled in a liquid-nitrogen stream at −173°C using a Rigaku X-stream 2000 cryosystem. The crystal from Crystal Screen 2 diffracted to a maximum resolution of 2.5 Å. Diffraction data were collected from a single cryoprotected crystal over a range of 360° with an oscillation angle of 1.0° and a crystal-to-detector distance of 175 mm. The second crystal from Index diffracted to 2.0 Å resolution. Diffraction data were collected with 0.5° oscillation over a range of 180° with a crystal-to-detector distance of 157 mm. Data were processed with *XDS* (Kabsch, 2010). Each data set was scaled in *SCALA* (Evans, 2006) and the presence of the screw axis was also confirmed by *POINTLESS* (Evans, 2006) in the *CCP*4 suite (Winn *et al.*, 2011).

3. Results and discussion

Sa-iPGM was successfully cloned in pQE30 expression vector, over-expressed in *E. coli* M15 (pREP4) cells and purified to homogeneity using Ni–NTA Sepharose and size-exclusion chromatography. The protein was crystallized in two different conditions: (i) 0.1 M HEPES pH 7.5, 20%(w/v) polyethylene glycol 10 000 (Fig. 1a) and (ii) 0.2 M NaCl, 0.1 M bis-tris pH 6.5, 25%(w/v) polyethylene glycol 3350 (Fig. 1b).

Crystals of His$_6$-iPGM obtained from both of the conditions were subjected to diffraction experiments. Diffraction data were collected using a cryoprotected single crystal from each of the crystallization conditions. The crystal from condition (i) diffracted to 2.5 Å resolution (Fig. 2a), and for those from condition (ii) the highest resolution limit was 2.0 Å (Fig. 2b). Analysis of crystal symmetry and systematic absences in the recorded diffraction patterns indicated that the crystals belonged to the orthorhombic space groups $P2_12_12$ and $P2_12_12_1$, respectively. The unit-cell parameters of crystal (i) were $a = 77.00, b = 86.11, c = 94.07$ Å and those of crystal (ii) were $a = 73.21, b = 81.75, c = 89.18$ Å. Determination of the Matthews coefficient suggests 55.5% ($V_M = 2.76$ Å^3 Da^{-1}) and 48.0% ($V_M = 2.36$ Å^3 Da^{-1})

solvent content in the unit cell for the $P2_12_12$ and $P2_12_12_1$ crystals, respectively, and both of them contained a single molecule in the asymmetric unit (Matthews, 1968). The overall completeness of the data set from the $P2_12_12$ crystal was 99.4%, with $R_{r.i.m.}$ = 14.9% and $CC_{1/2}$ = 99.9. For the $P2_12_12_1$ crystal, $R_{r.i.m.}$ was 9.0% and $CC_{1/2}$ was 99.9, with an overall completeness of 99.3%. The data-collection and processing statistics are given in Table 1.

The structure has been solved by the molecular-replacement method using homologous crystal structures of iPGM. Initial molecular-

replacement trials failed to extract the phase information from the templates (PDB entries 1ejj and 2ify; Jedrzejas et al., 2000; Nukui et al., 2007), which had a sequence homology of above 50%. This may be owing to different orientations of the two domains in the structure or to the physico-chemical state in the crystallization. To solve the problem, two domains were used as separate ensembles in the molecular-replacement process using Phaser (McCoy et al., 2007) in the PHENIX platform (Adams et al., 2010). Ensemble 1 was composed of 272 amino acids (Lys3–Val75 and Val306–Thr504 of PDB entry 1ejj), while 206 amino acids (Asp91–His206 of PDB entry 2ify) were present in ensemble 2. Molecular replacement suggested the presence of one molecule in the asymmetric unit, and the self-rotation function peak generated by MOLREP (Vagin & Teplyakov, 2010) also concluded that there was only one molecule in the asymmetric unit for both of the crystals (Fig. 3). Model building and successive refinement cycles are currently in progress.
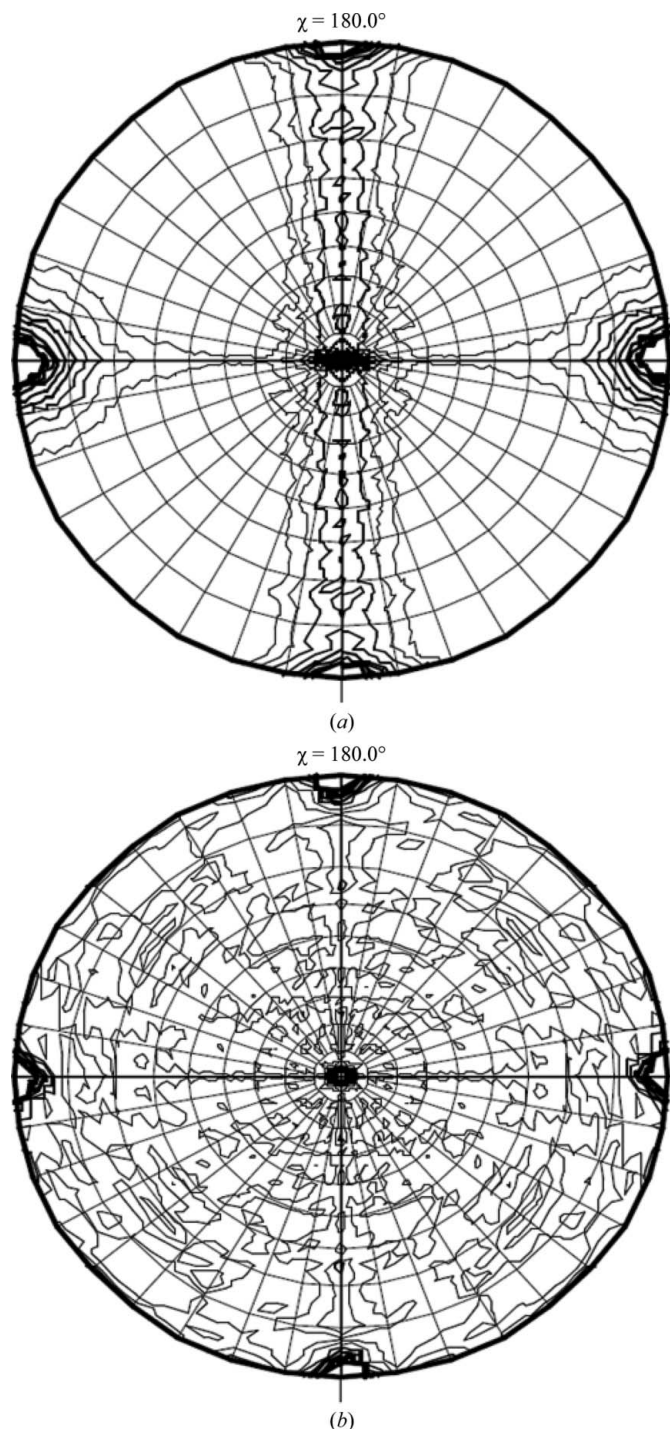
Figure 3
The self-rotation function plots of (a) crystal (i) and (b) crystal (ii) suggest that both of them have P222 symmetry and the absence of any off-origin peak suggests the presence of one molecule in the asymmetric unit of each crystal.

References

Adams, P. D. et al. (2010). Acta Cryst. D66, 213–221.
Archer, G. L. (1998). Clin. Infect. Dis. 26, 1179–1181.
Becker, P., Hufnagle, W., Peters, G. & Herrmann, M. (2001). Appl. Environ. Microbiol. 67, 2958–2965.
Bradford, M. M. (1976). Anal. Biochem. 72, 248–254.
Evans, P. (2006). Acta Cryst. D62, 72–82.
Götz, F. (2002). Mol. Microbiol. 43, 1367–1378.
Jedrzejas, M. J., Chander, M., Setlow, P. & Krishnasamy, G. (2000). EMBO J. 19, 1419–1431.
Kabsch, W. (2010). Acta Cryst. D66, 125–132.
Kuhn, N. J., Setlow, B., Setlow, P., Cammack, R. & Williams, R. (1995). Arch. Biochem. Biophys. 320, 35–42.
MacGregor, J. S., Singh, V. N., Davoust, S., Melloni, E., Pontremoli, S. & Horecker, B. L. (1980). Proc. Natl Acad. Sci. USA, 77, 3889–3892.
Magill, N. G., Cowan, A. E., Koppel, D. E. & Setlow, P. (1994). J. Bacteriol. 176, 2252–2258.
Magill, N. G., Cowan, A. E., Leyva-Vazquez, M. A., Brown, M., Koppel, D. E. & Setlow, P. (1996). J. Bacteriol. 178, 2204–2210.
Matthews, B. W. (1968). J. Mol. Biol. 33, 491–497.
McCoy, A. J., Grosse-Kunstleve, R. W., Adams, P. D., Winn, M. D., Storoni, L. C. & Read, R. J. (2007). J. Appl. Cryst. 40, 658–674.
Mukherjee, S., Dutta, D., Saha, B. & Das, A. K. (2010). J. Mol. Biol. 401, 949–968.
Mukherjee, S., Roychowdhury, A., Dutta, D. & Das, A. K. (2012). Biochimie, 94, 2532–2544.
Nukui, M., Mello, L. V., Littlejohn, J. E., Setlow, B., Setlow, P., Kim, K., Leighton, T. & Jedrzejas, M. J. (2007). Biophys. J. 92, 977–988.
Ovádi, J. & Keleti, T. (1978). Eur. J. Biochem. 85, 157–161.
Purves, J., Cockayne, A., Moody, P. C. E. & Morrissey, J. A. (2010). Infect. Immun. 78, 5223–5232.
Roychowdhury, A., Mukherjee, S. & Das, A. K. (2011). Acta Cryst. F67, 668–671.
Schurig, H., Beaucamp, N., Ostendorp, R., Jaenicke, R., Adler, E. & Knowles, J. R. (1995). EMBO J. 14, 442–451.
Vagin, A. & Teplyakov, A. (2010). Acta Cryst. D66, 22–25.
Weber, J. P. & Bernhard, S. A. (1982). Biochemistry, 21, 4189–4194.
Winn, M. D. et al. (2011). Acta Cryst. D67, 235–242.